SUPPLEMENTARY MATERIAL

SUPP FIGURE 1

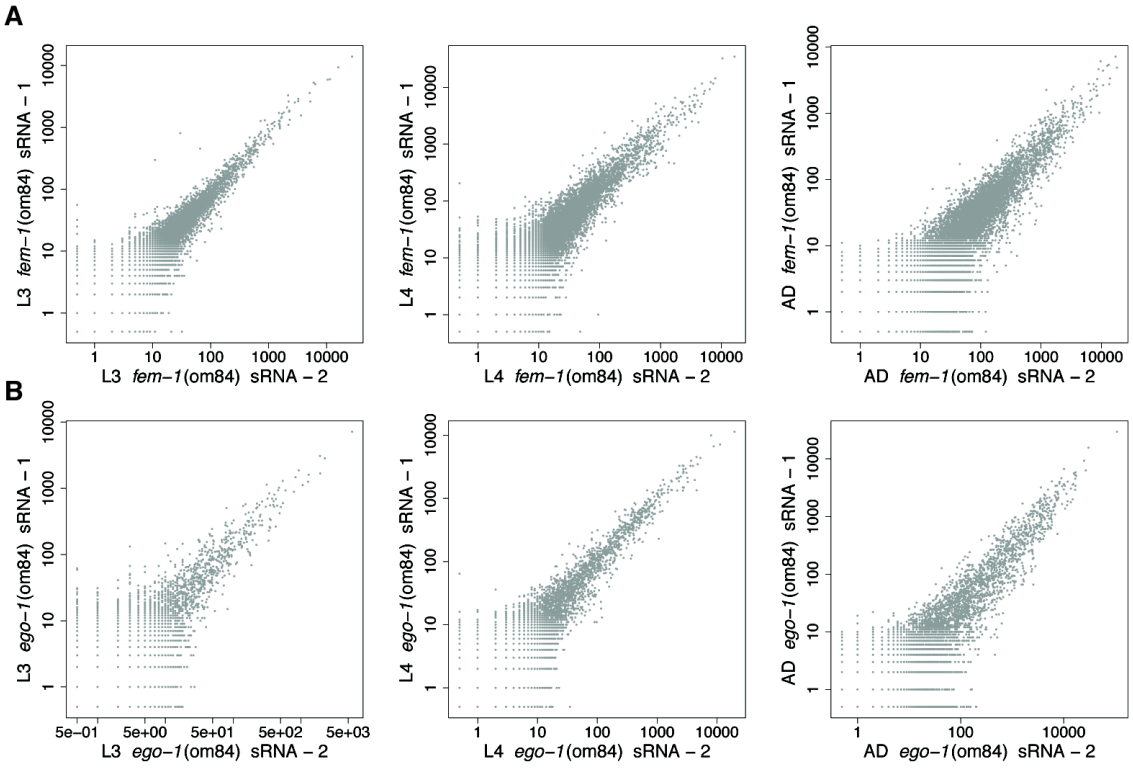

Supplementary Figure 1. Scatter plots depict a gene-by-gene comparison of small RNA abundance for equivalent stage and genotype. **(A)** *fem-1(hc17)*. **(B)** *ego-1(om84)*; *fem-1(hc17)*.

SUPP FIGURE 2

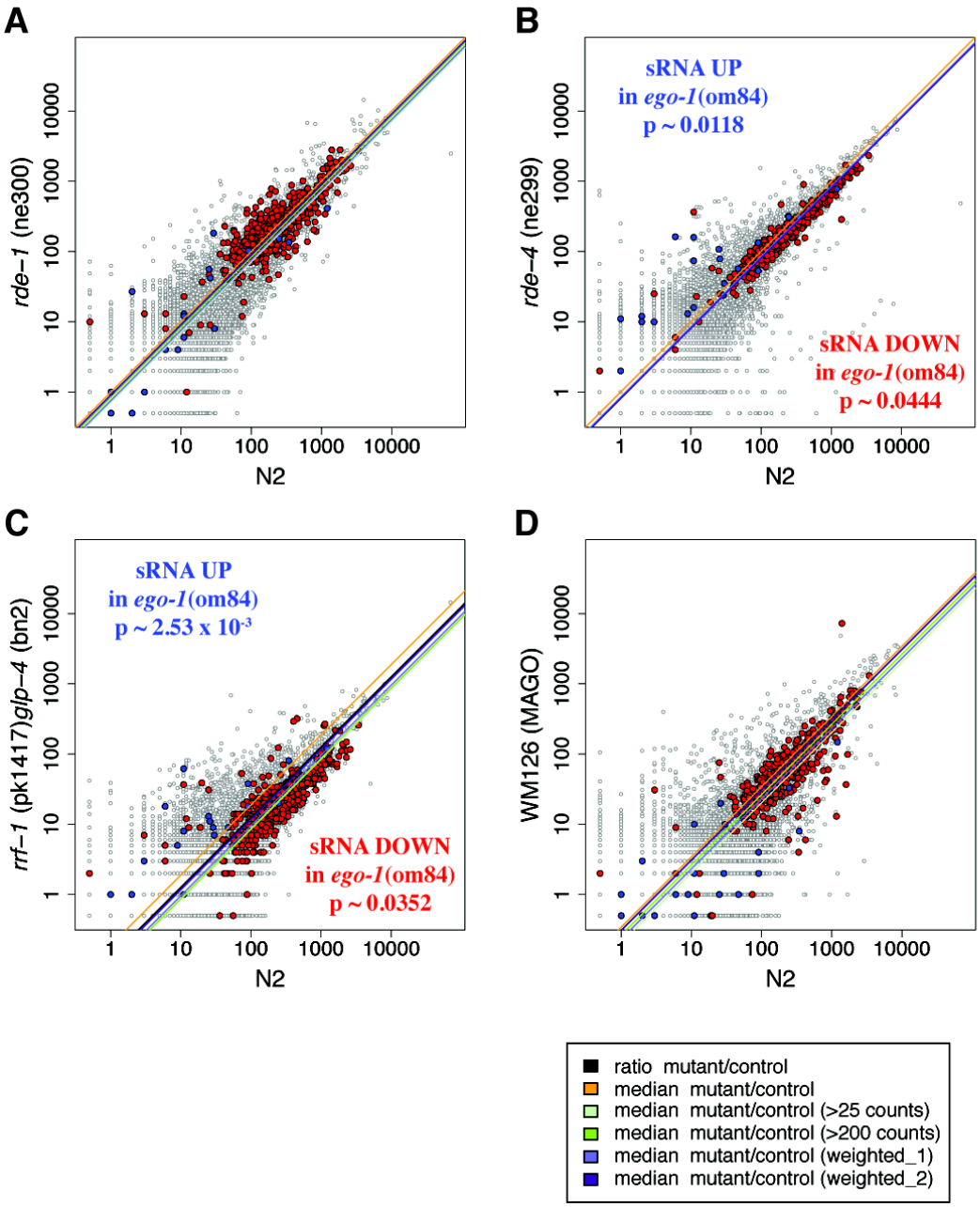

SUPP FIGURE 2 (cont.)

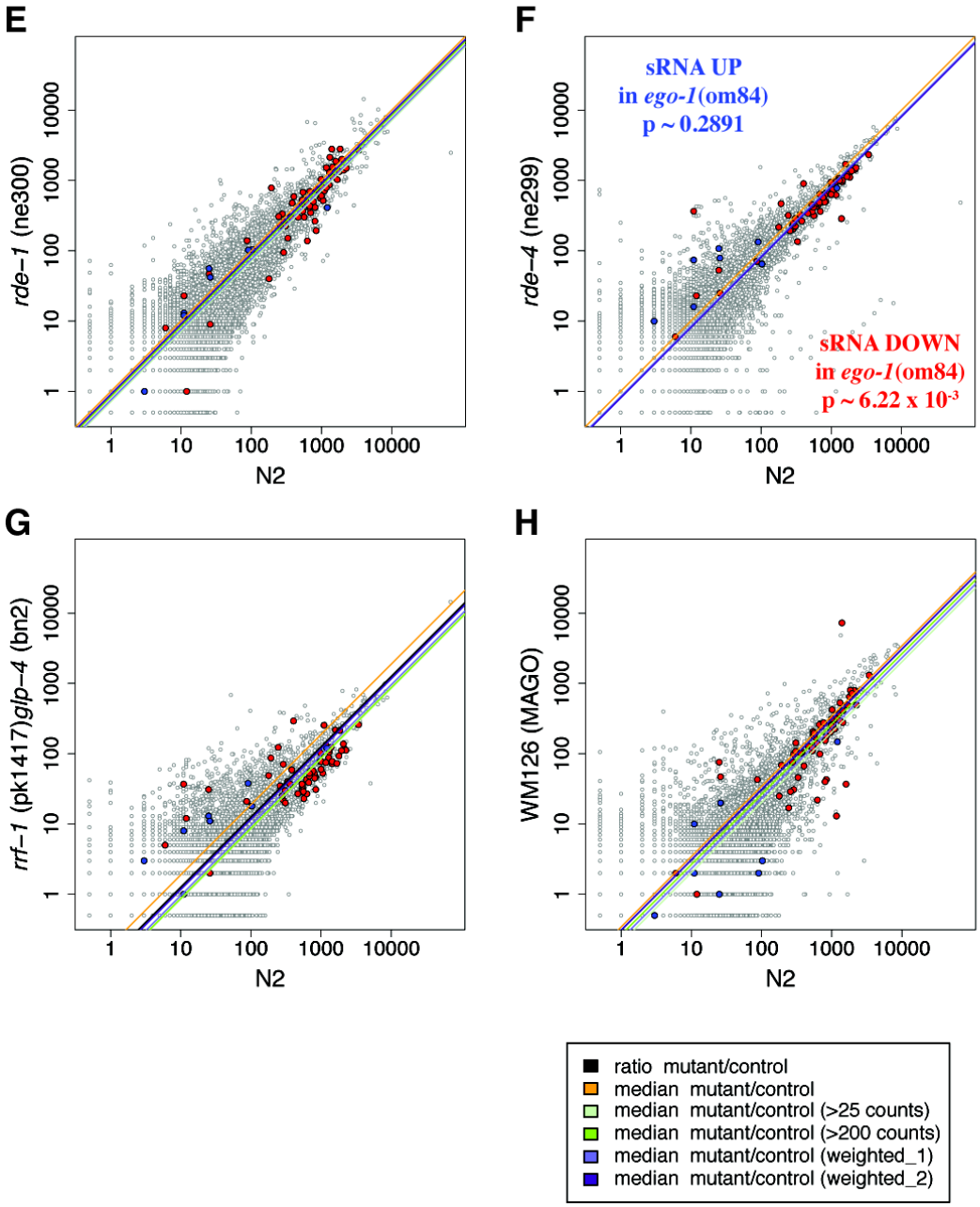

SUPP FIGURE 2 (cont.)

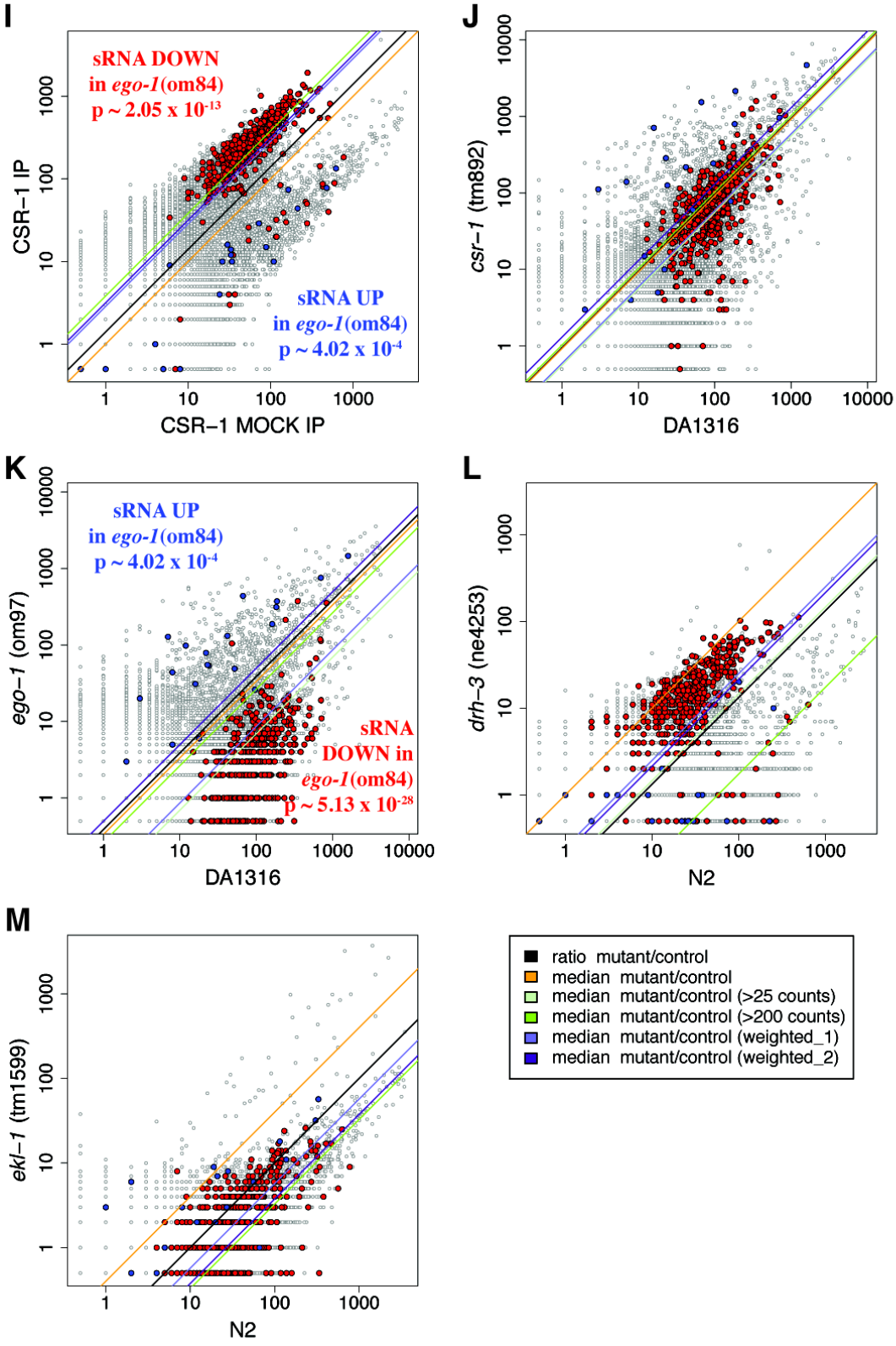

SUPP FIGURE 2 (cont.)

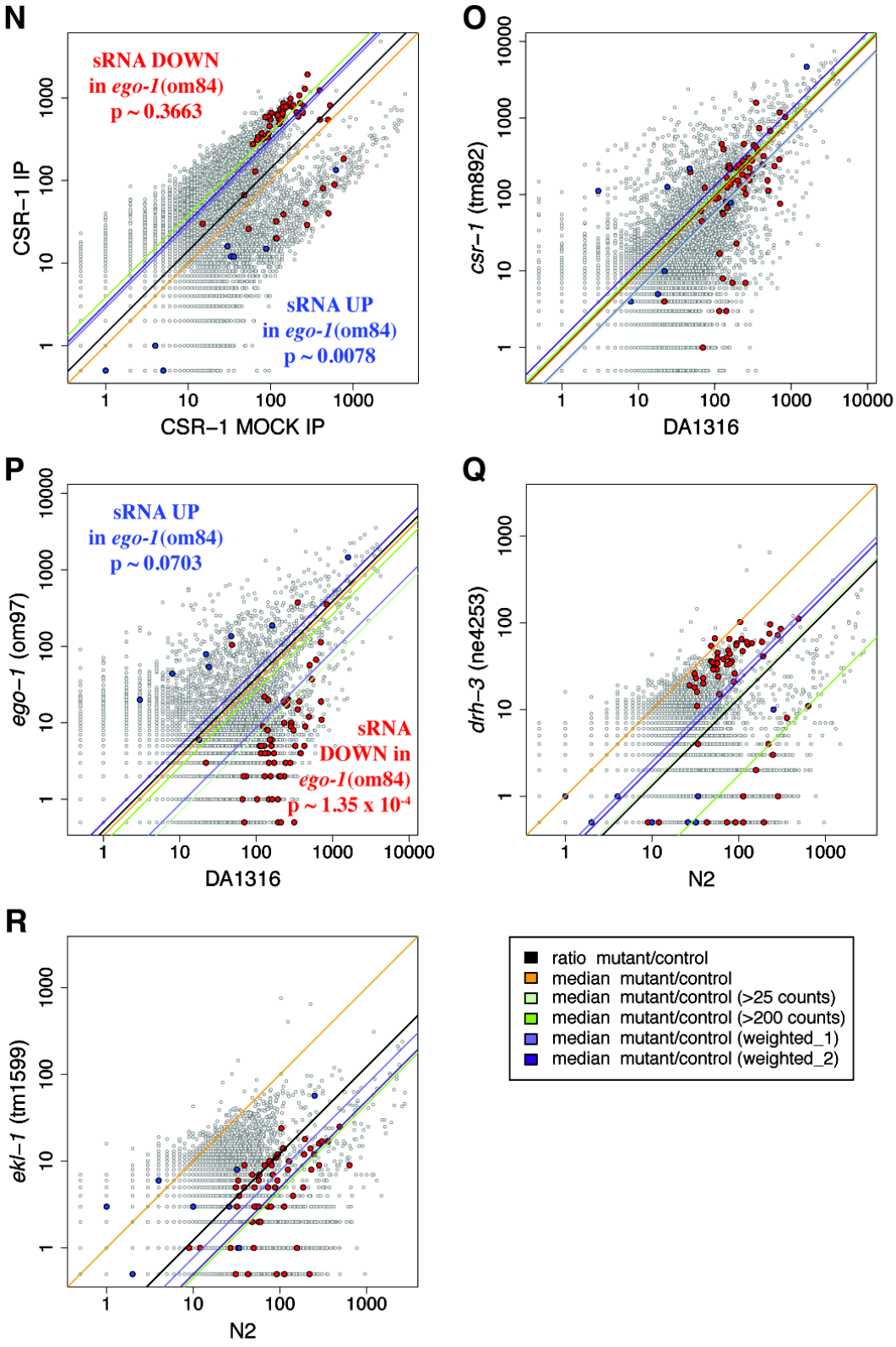

SUPP FIGURE 2 (cont.)

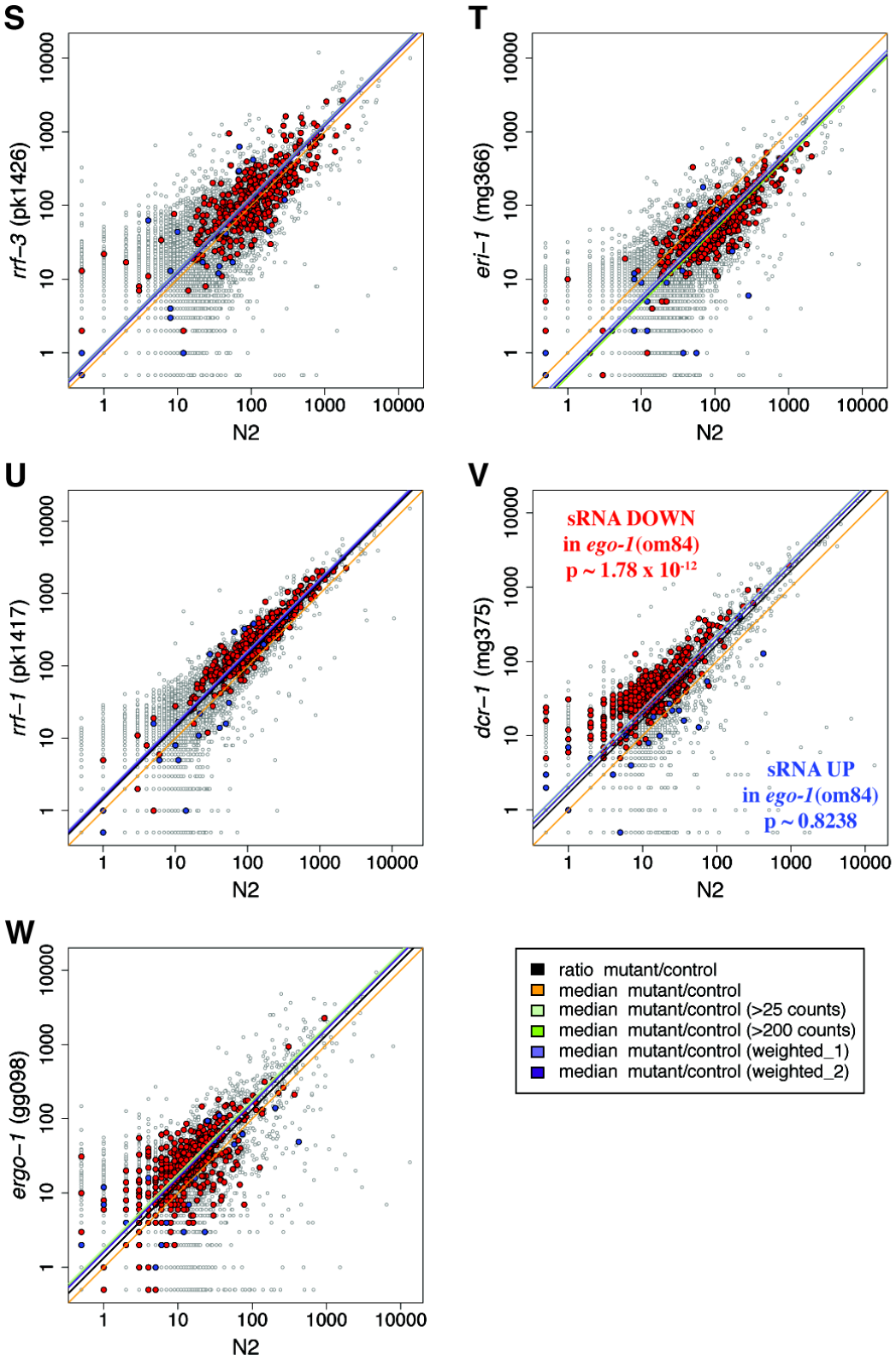

SUPP FIGURE 2 (cont.)

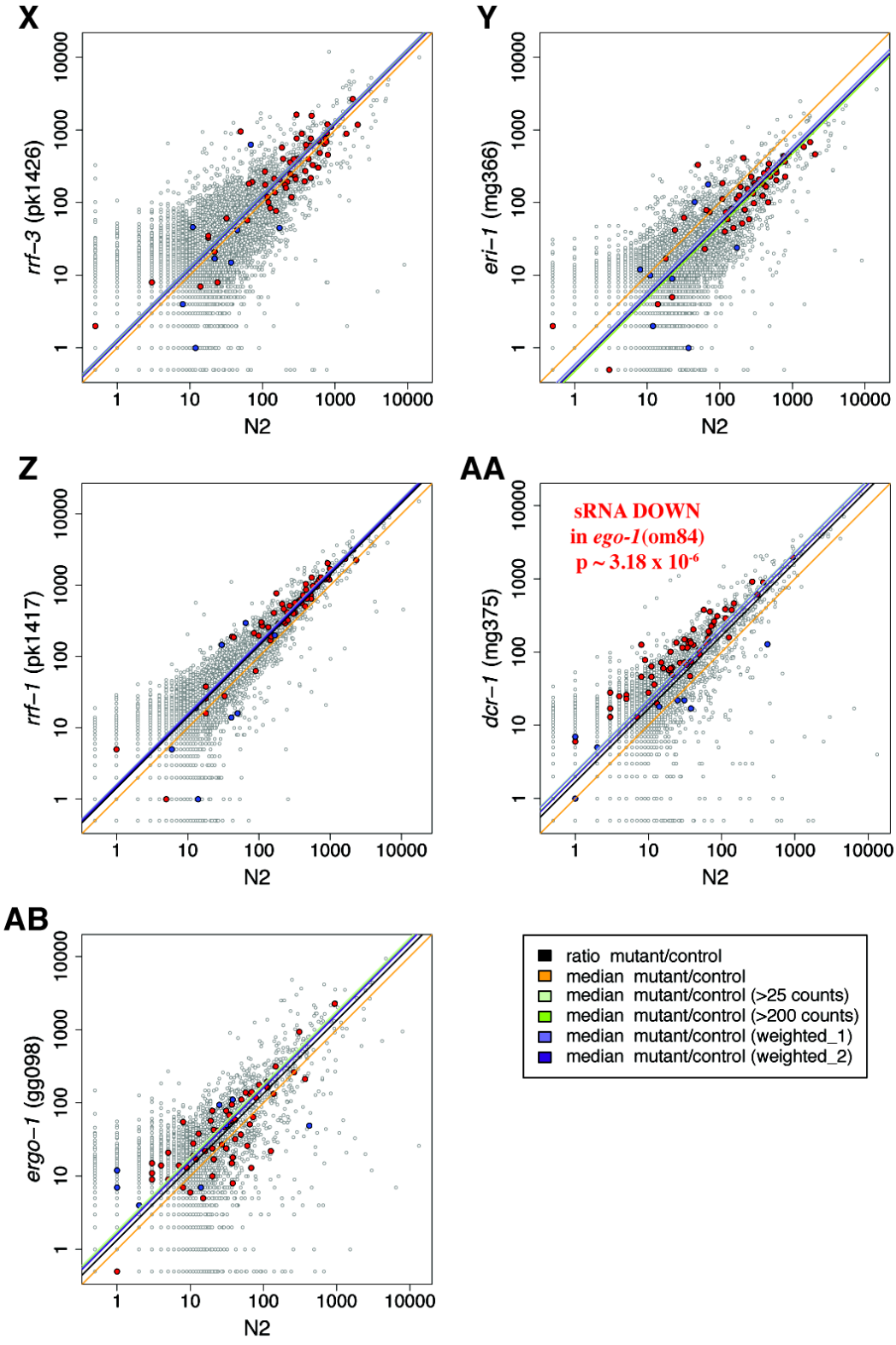

Supplementary Figure 2. Genetic requirements for EGO-1 target accumulation. Scatter plots depict a gene-by-gene comparison of small RNA abundance for several RNAi-related genes. Highlighted are genes whose 5'-independent sRNA abundance is down in L4/adult (and L3/L4/adult) *ego-1(om84)* (sRNA DOWN, red) and genes whose 5'-independent sRNA abundance is up in L4/adult (L3/L4/adult) *ego-1(om84)* (sRNA UP, blue). We determined a series of median ratios (see Methods) and used the most conservative in each case to calculate p-values based on the location of red and blue points relative to those medians. **(A)** L4/AD: *rde-1(ne300)*. No significant shift. **(B)** L4/AD: *rde-4(ne299)*. 240 of 437 sRNA DOWN genes fall below the lowest median ratio (p-value ~ 0.05) and 16 of 20 sRNA UP genes fall above the highest median ratio (p-value ~ 0.02). **(C)** L4/AD: *rrf-1(pk1417) glp-4(bn2)*. 241 of 437 sRNA DOWN genes fall below the lowest median ratio (p-value ~ 0.04) and 17 of 20 sRNA UP genes fall above the highest median ratio (p-value ~ 2.53×10^{-3}). **(D)** L4/AD: WM126 (MAGO). No significant shift. **(E)** L3/L4/AD: *rde-1(ne300)*. No significant shift. **(F)** L3/L4/AD: *rde-4(ne299)*. 41 of 60 sRNA DOWN genes fall below the lowest median ratio (p-value ~ 6.22×10^{-3}) and 6 of 8 sRNA UP genes fall above the highest median ratio (p-value ~ 0.2891). **(G)** L3/L4/AD: *rrf-1(pk1417) glp-4(bn2)*. No significant shift. **(H)** L3/L4/AD: WM126 (MAGO). No significant shift. **(I)** L4/AD: CSR-1:IP. We found that 295 of 437 sRNA DOWN genes are enriched in CSR-1 complexes (p-value ~ 2.05×10^{-13}) and 18 of 20 sRNA UP genes (p-value ~ 4.02×10^{-4}) fall below the lowest median value in CSR-1:IP sequencing data. **(J)** L4/AD: *csr-1(tm892)*. No significant shift. **(K)** L4/AD: *ego-1(om97)*. We found that 331 of 437 L4/adult EGO-1 targets (red) found in *ego-1(om84)* fall below the lowest median ratio (p-value ~ 5.13×10^{-28}) and 18 of 20 genes whose

sRNA counts increase significantly in *ego-1(om84)* (blue) fall above the greatest median ratio in *ego-1(om97)* (p-value ~ 4.02×10^{-4}). **(L)** L4/AD: *drh-3(ne4253)*. No significant shift. **(M)** L4/AD: *ekl-1(tm1599)*. No significant shift. **(N)** L3/L4/AD: CSR-1:IP. We found that 34 of 60 sRNA DOWN genes are enriched in CSR-1 complexes (p-value ~ 0.3663) and 8 of 8 sRNA UP genes (p-value ~ 0.0078) fall below the lowest median value in CSR-1:IP sequencing data. **(O)** L3/L4/AD: *csr-1(tm892)*. No significant shift. **(P)** L3/L4/AD: *ego-1(om97)*. We found that 45 of 60 L3/L4/adult EGO-1 targets (red) found in *ego-1(om84)* fall below the lowest median ratio (p-value ~ 1.35×10^{-4}) and 7 of 8 genes whose sRNA counts increase significantly in ego-1(om84) (blue) fall above the greatest median ratio in ego-1(om97) (p-value ~ 0.0703). **(Q)** L3/L4/AD: *drh-3(ne4253)*. No significant shift. **(R)** L3/L4/AD: *ekl-1(tm1599)*. No significant shift. **(S)** L4/AD: *rrf-3(pk1426)*. No significant shift. **(T)** L4/AD: *eri-1(mg366)*. No significant shift. **(U)** L4/AD: *rrf-1(pk1417)*. No significant shift. **(V)** L4/AD: *dcr-1(mg375)*. 292 of 437 sRNA DOWN genes fall above the highest median ratio (p-value ~ 1.79×10^{-12}). **(W)** L4/AD: *ergo-1(gg098)*. No significant shift. **(X)** L3/L4/AD: *rrf-3(pk1426)*. No significant shift. **(Y)** L3/L4/AD: *eri-1(mg366)*. No significant shift. **(Z)** L3/L4/AD: *rrf-1(pk1417)*. No significant shift. **(AA)** L3/L4/AD: *dcr-1(mg375)*. 48 of 60 sRNA DOWN genes fall above the highest median ratio (p-value ~ 3.18×10^{-6}). **(AB)** L3/L4/AD: *ergo-1(gg098)*. No significant shift.

SUPP FIGURE 3

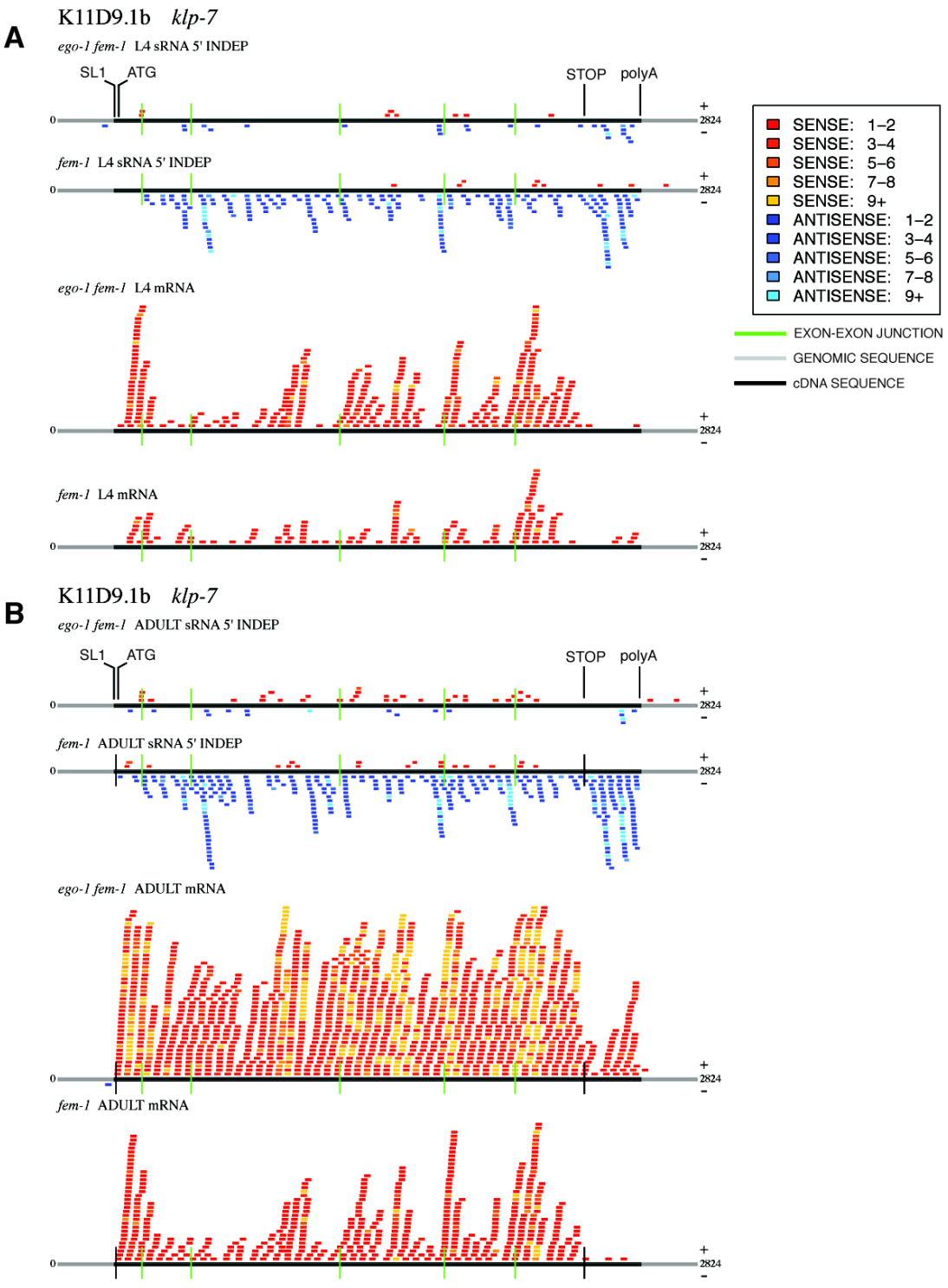

SUPP FIGURE 3 (cont.)

C

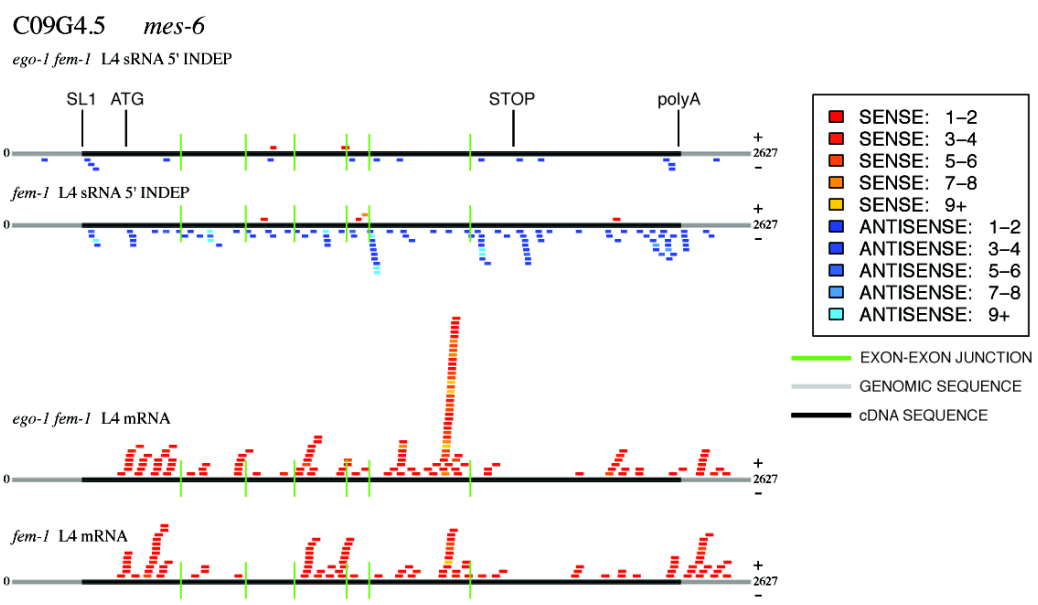

D

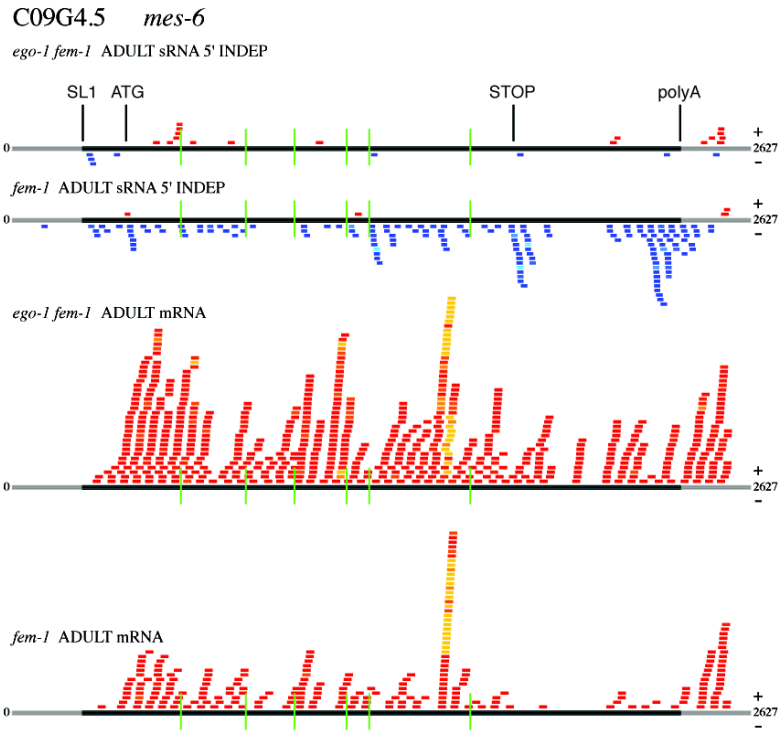

SUPP FIGURE 3 (cont.)

E

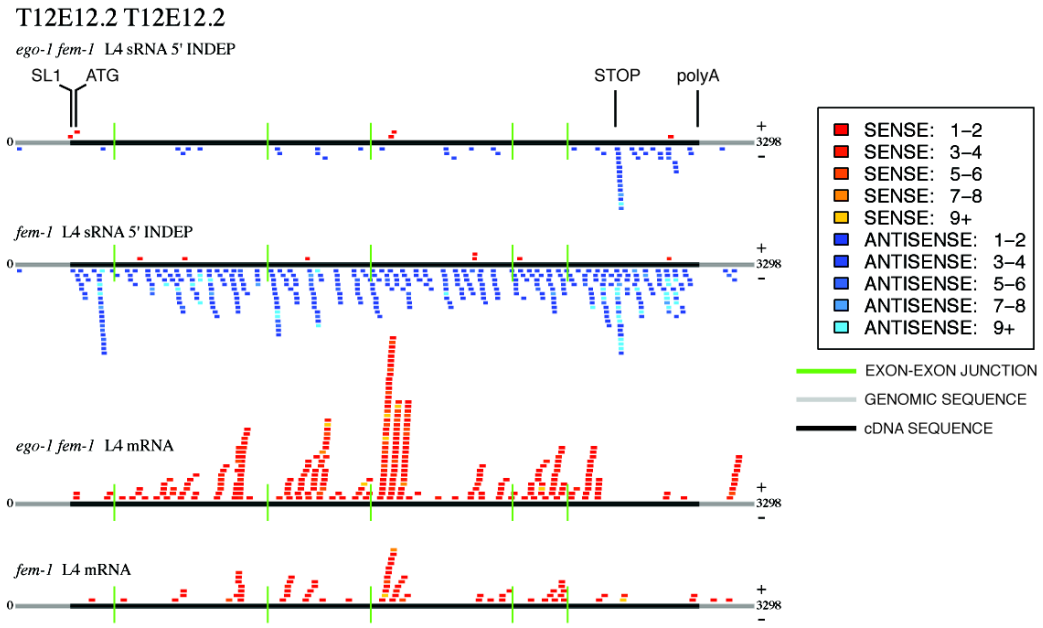

F

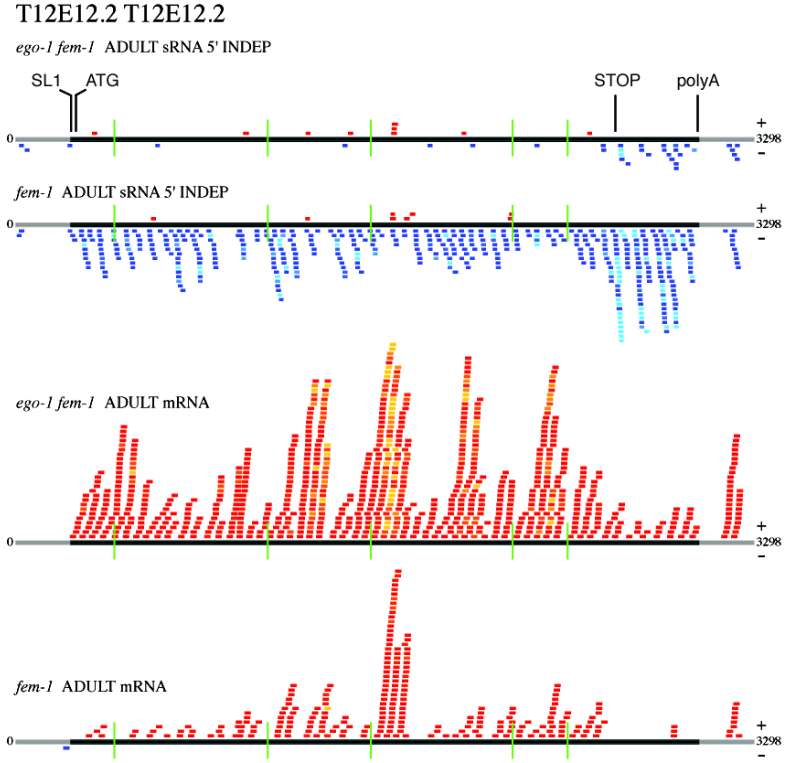

Supplementary Figure 3. Small RNA and mRNA sequencing reads of *klp-7, mes-6,* T12E12.2. Sense (shades of red) and antisense (shades of blue) reads of 5'-independent small RNAs and mRNA [experimental: *ego-1(om84) fem-1(hc17)* and control: *fem-1(hc17)*] mapped to spliced transcripts. **(A)** *klp-7* - L4-staged animals. **(B)** *klp-7* - Adult-staged animals. **(C)** *mes-6* - L4-staged animals. **(D)** *mes-6* - Adult-staged animals. **(E)** T12E12.3 - L4-staged animals. **(F)** T12E12.2 - Adult-staged animals.

SUPP FIGURE 4

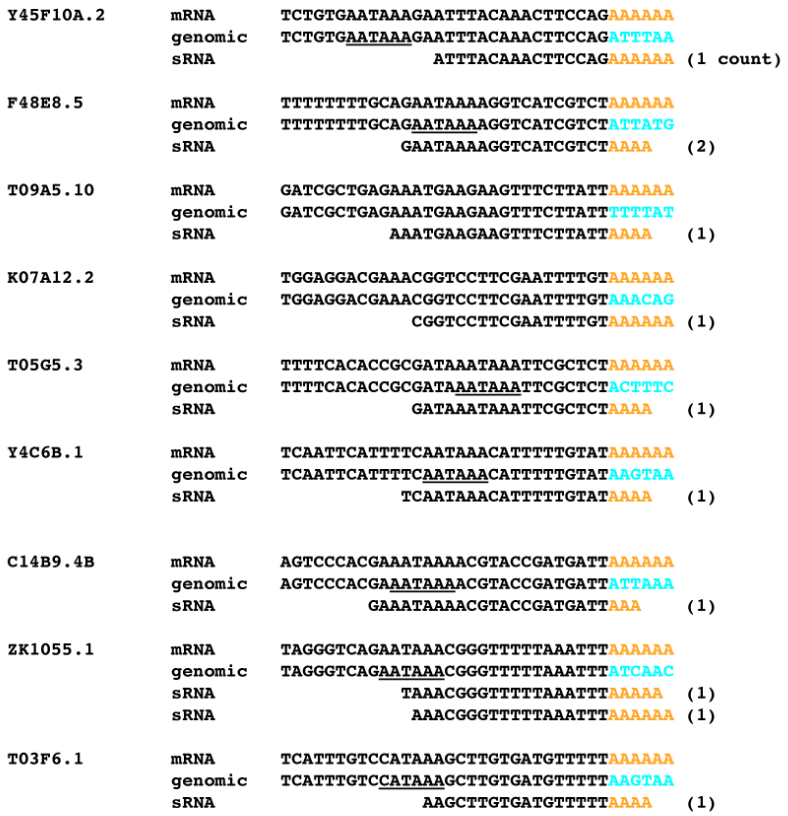

Supplementary Figure 4. Small RNAs that span mRNA-polyA junctions. We found 10 independent small RNAs (antisense to 9 putative EGO-1 targets) that span the 3'UTR-polyA junction in *fem-1(hc17)* control samples. Each of these contained the 3' linker sequence downstream of the nucleotides shown, with each defined by reads with Illumina GA2 quality scores of at least 32 (on a -5 to 40 scale). No mRNA-polyA junction RNAs for putative L4/Adult EGO-1 targets were found in experimental *ego-1(om84)*; *fem-1(hc17)* animals. The polyadenlyation signal has been underlined for each gene.

SUPP FIGURE 5

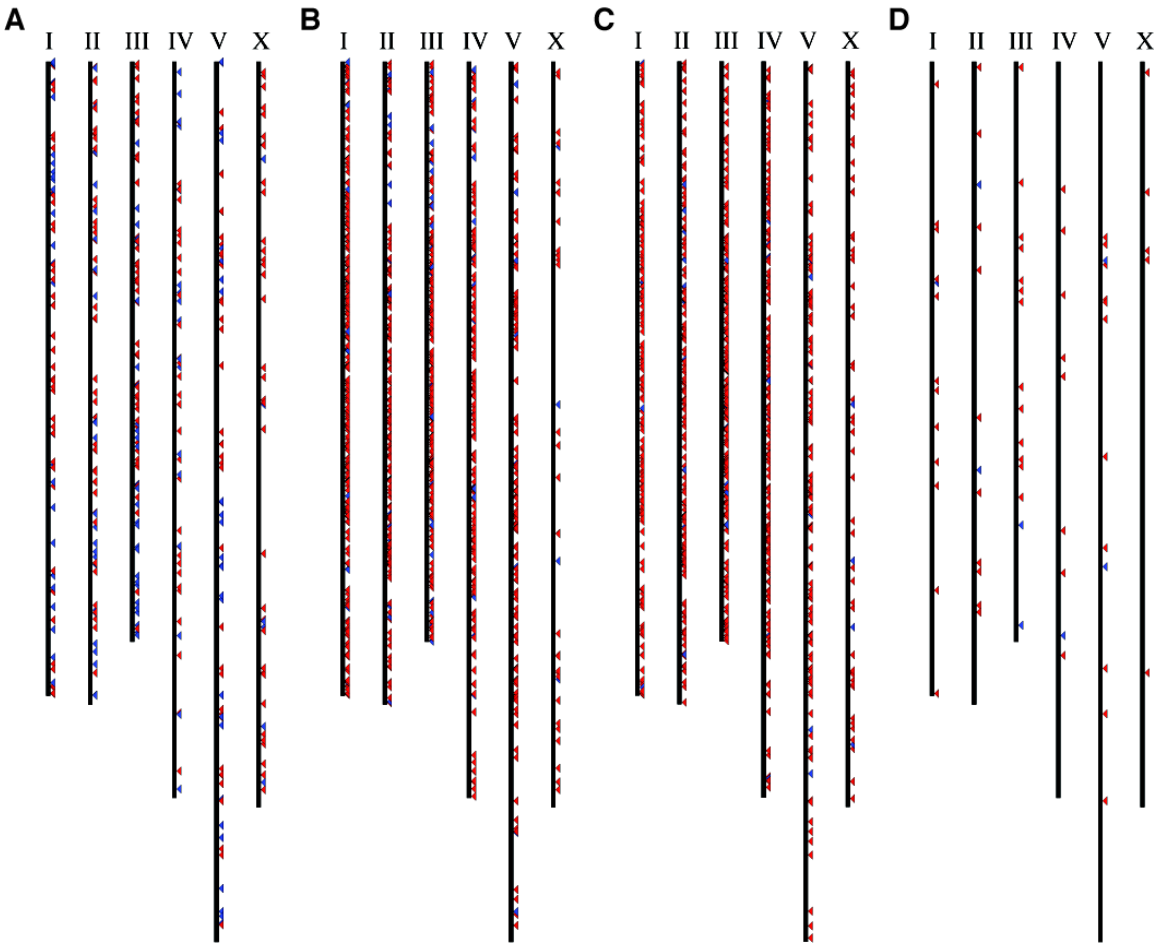

Supplementary Figure 5. Chromosomal positions of EGO-1 targets. Chromosome size and gene positions are drawn to scale. **(A)** L3. Genes whose small RNA abundance is decreased 2-fold [red, DOWN] or increased 2-fold [blue, UP] in *ego-1(om84)* relative to *ego-1(+)* with a posterior probability ratio [PPR] < 0.005. [I] 41 genes DOWN, 30 genes UP. [II] 47 genes DOWN, 27 genes UP. [III] 50 genes DOWN, 31 genes UP. [IV] 32 genes DOWN, 20 genes UP. [V] 36 genes DOWN, 31 genes UP. [X] 37 genes DOWN, 6 genes UP. **(B)** L4. Genes whose small RNA abundance is decreased 3-fold [red, DOWN] or increased 3-fold [blue, UP] in *ego-1(om84)* relative to *ego-1(+)* with a [PPR] < 0.005. [I] 262 genes DOWN, 20 genes UP. [II] 190 genes DOWN, 26 genes UP. [III] 247 genes DOWN, 34 genes UP. [IV] 192 genes DOWN, 18 genes UP. [V] 142 genes DOWN, 13 genes UP. [X] 33 genes DOWN, 4 genes UP. **(C)** Adult. Genes whose small RNA abundance is decreased 3-fold [red, DOWN] or increased 3-fold [blue, UP] in *ego-1(om84)* relative to *ego-1(+)* with a [PPR] < 0.005. [I] 186 genes DOWN, 6 genes UP. [II] 165 genes DOWN, 13 genes UP. [III] 188 genes DOWN, 10 genes UP. [IV] 163 genes DOWN, 10 genes UP. [V] 127 genes DOWN, 8 genes UP. [X] 51 genes DOWN, 4 genes UP. **(D)** L3, L4, and adult. Genes whose small RNA abundance is decreased 3-fold [red, DOWN] or increased 3-fold [blue, UP] in *ego-1(om84)* relative to *ego-1(+)* with a [PPR] < 0.005 (2-fold in L3. [I] 12 genes DOWN, 1 genes UP. [II] 10 genes DOWN, 2 genes UP. [III] 14 genes DOWN, 2 genes UP. [IV] 8 genes DOWN, 1 gene UP. [V] 11 genes DOWN, 2 genes UP. [X] 5 genes DOWN, 0 genes UP. We found only 33 putative EGO-1 targets (of 1066 total targets) to be on the X chromosome in L4 datasets (p-value ~ 7.83×10^{-34}). We also found that only 51 putative EGO-1 targets (880 total) to be on the X chromosome in adult datasets (p-value ~ 5.35×10^{-15}).

Correcting for multiple hypotheses, we found that EGO-1 targets are significantly underrepresented on the X chromosome.

SUPP FIGURE 6

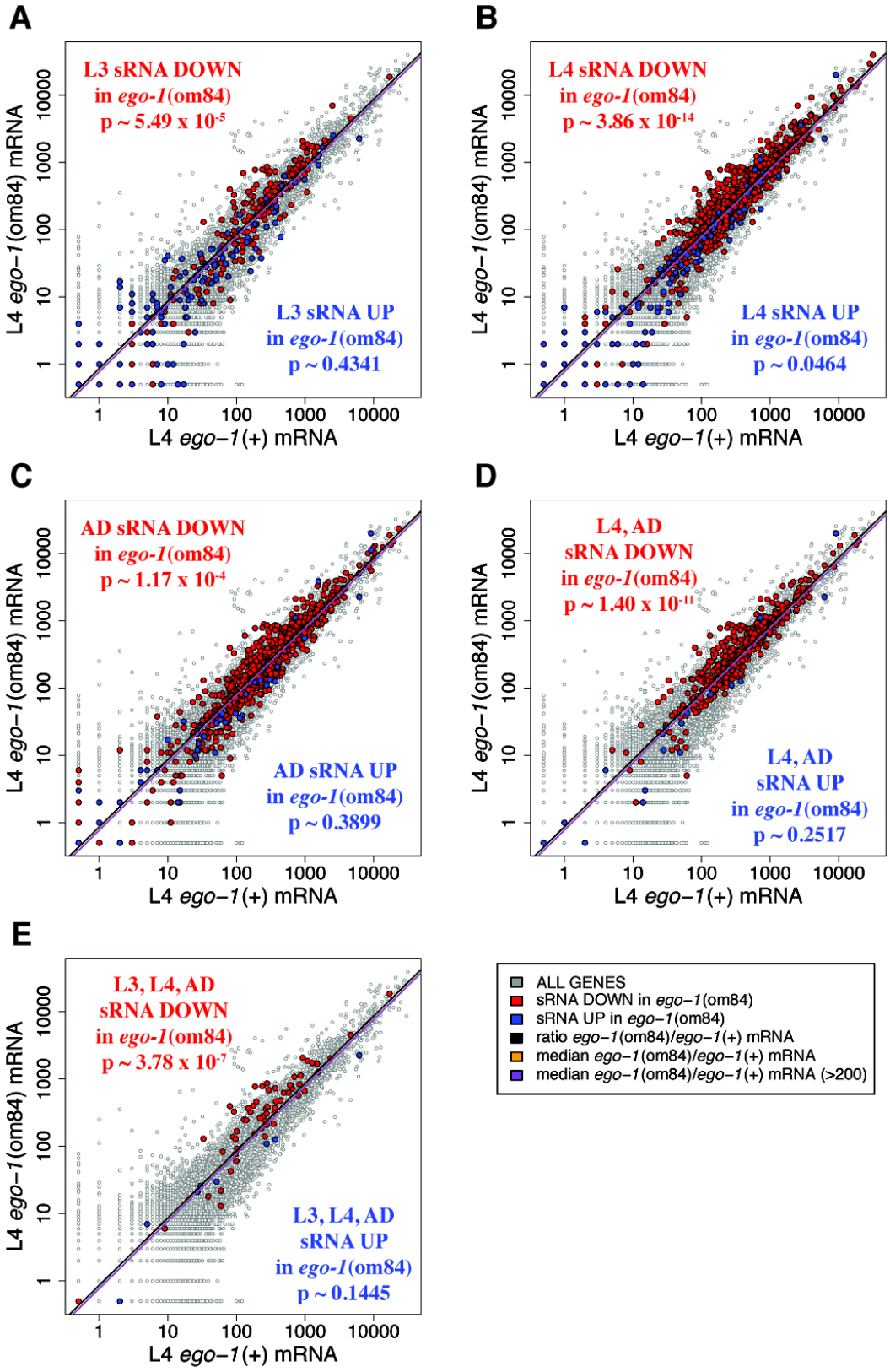

SUPP FIGURE 6 (cont.)

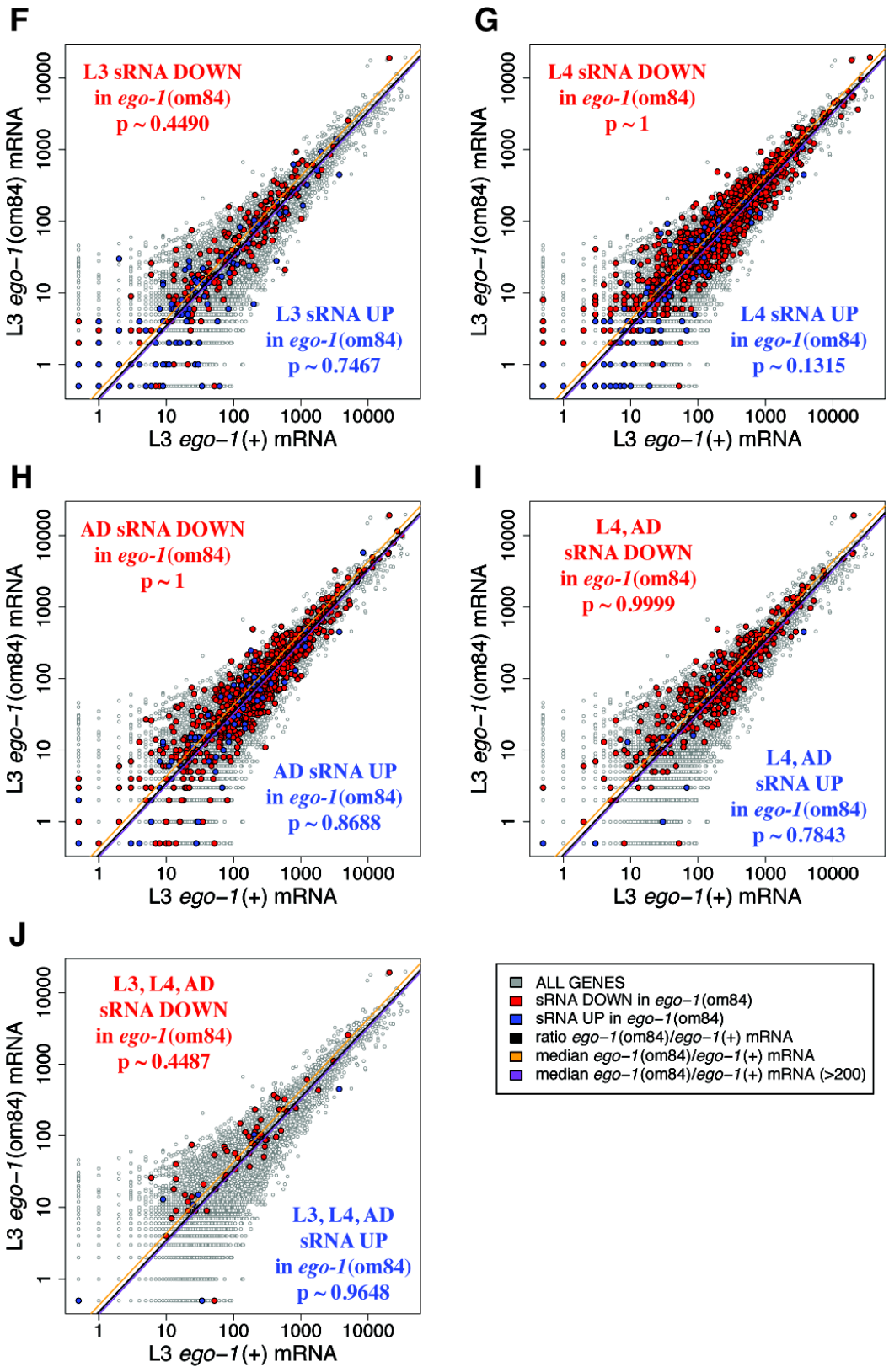

Supplementary Figure 6. Summary of L4 and L3 mRNA abundance. Scatter plots depict a gene-by-gene comparison of mRNA abundance in staged L4 and L3 animals (gray), and highlighted are genes whose sRNA abundance is down in *ego-1(om84)* (red) and genes whose sRNA abundance is up in *ego-1(om84)* (blue). As the key question for these data was the existence of an inverse relationship between small RNA (sRNA) and mRNA abundance, a central aspect of the data is the median values of the ratio of mRNA levels in *ego-1(om84)*/mRNA levels in *ego-1(+)*. Two median lines are shown for each dataset: (i) median of the ratio of *ego-1(om84)*/*ego-1(+)* on a gene-by-gene basis (ii) median of the ratio of *ego-1(om84)*/*ego-1(+)* on a gene-by-gene basis using only those genes for which the sum of *ego-1(om84)* and *ego-1(+)* counts is greater than 200. A black line shows the total ratio of total counts in each pair of samples giving the expected parity between samples. Gene counts summary: **(A)** L4 mRNA: Changes in L3 sRNA abundance: 243 genes down 2-fold (red, p-value ~ 5.49×10^{-5}) and 145 genes up 2-fold (blue, p ~ 0.4341). **(B)** L4 mRNA: Changes in L4 sRNA abundance: 1066 genes down 3-fold (red, p-value ~ 3.86×10^{-14}) and 115 genes up 3-fold (blue, p ~ 0.0464). **(C)** L4 mRNA: Changes in adult sRNA abundance: 880 genes down 3-fold (red, p-value ~ 1.17×10^{-4}) and 51 genes up 3-fold (blue, p ~ 0.3899). **(D)** L4 mRNA: Changes in L4 and adult sRNA abundance: 437 genes down 3-fold (red, p-value ~ 1.40×10^{-11}) and 20 genes up 3-fold (blue, p ~ 0.2517). **(E)** L4 mRNA: Changes in L3, L4, and adult sRNA abundance: 60 genes down 2-fold in L3 and 3-fold in L4 and adult (red, p-value ~ 3.78×10^{-7}) and 115 genes up (blue, p ~ 0.1445). **(F)** L3 mRNA: Changes in L3 sRNA abundance: 243 genes down 2-fold (red, p-value ~ 0.4490) and 145 genes up 2-fold (blue, p ~ 0.7467). **(G)** L3 mRNA: Changes in L4 sRNA abundance: 1066 genes down 3-fold

(red, p-value ~ 1) and 115 genes up 3-fold (blue, p ~ 0.1315). **(H)** L3 mRNA: Changes in adult sRNA abundance: 880 genes down 3-fold (red, p-value ~ 1) and 51 genes up 3-fold (blue, p ~ 0.8688). **(I)** L3 mRNA: Changes in L4 and adult sRNA abundance: 437 genes down 3-fold (red, p-value ~ 0.9999) and 20 genes up 3-fold (blue, p ~ 0.7843). **(J)** L3 mRNA: Changes in L3, L4, and adult sRNA abundance: 60 genes down 2-fold in L3 and 3-fold in L4 and adult (red, p-value ~ 0.4487) and 115 genes up (blue, p ~ 0.9648).

SUPP TABLE 1

Attached as EXCEL file: ego-1_sRNA_L4_AD_table.xls

Supplementary Table 1. EGO-1 small RNA targets in L4 and adult worms. 437 genes were found to have at least 3-fold fewer small RNAs (posterior probability < 0.005) in L4 and adult *ego-1(om84)* worms. 20 genes were found to have at least 3-fold more small RNAs (posterior probability < 0.005) in L4 and adult *ego-1(om84)* worms.

SUPP TABLE 2

Attached as EXCEL file: ego-1_sRNA_L3_L4_AD_table.xls

Supplementary Table 2. EGO-1 small RNA targets in L3, L4, and adult worms. 60 genes were found to have at least 3-fold fewer small RNAs in L4 and adult and at least 2-fold fewer small RNAs in L3 (posterior probability < 0.005) in *ego-1(om84)* worms. 8 genes were found to have at least 3-fold more small RNAs in L4 and adult and at least 2-fold fewer more RNAs in L3 (posterior probability < 0.005) in *ego-1(om84)* worms.

SUPP TABLE 3

Attached as EXCEL file: ego-1_sRNA_L4_AD_table_less_stringent.xls

Supplementary Table 3. EGO-1 small RNA targets in L4 and adult worms. Using only 2 adult sample pairs (JMM-cel-009/012 and JMM-cel-011/014) we found 965 genes to have at least 3-fold fewer small RNAs (posterior probability < 0.005) in L4 and adult *ego-1(om84)* worms. We found 35 genes to have at least 3-fold more small RNAs (posterior probability < 0.005) in L4 and adult *ego-1(om84)* worms.

EXPERIMENTAL PROCEDURES

Worm strains

N2

PD8811 *ego-1(om84) unc-29(e193)*/hT2[qIS48] I; +/hT2[qIS48] III

PD8813 *ego-1(om84) unc-29(e193)*/ccIs4251 *egl-31(n472)* I

PD8826 *ego-1(om84) unc-29(e193)*/hT2[qIS48] I; +/hT2[qIS48] III ; *fem-1(hc17)* IV

PD8827 *unc-29(e193)* I; *fem-1(hc17)* IV

BA17 *fem-1(hc17)* IV

CB193 *unc-29(e193)* I

EL391 *ego-1(om84) unc-29(e193)*/hT2[*dpy-18(h662)*] I; +/hT2[*bli-4(e937)*] III

Worm growth, synchronization and isolation

All strains used in sRNA and mRNA sequencing were synchronized by treating gravid adults with a 5.25% hypochlorite solution to kill all stages except embryos. Embryos were grown on enriched-peptone plates (20 g/L) at 25°C to L3, L4 and adult stages. *ego-1(-) unc-29(-) fem-1(-)* mutant and *unc-29(-) fem-1(-)* control animals were isolated by treating synchronized populations of PD8826 and PD8827 with a 2mM levamisole solution for 10 minutes. The animals were then placed on the non-seeded half of an enriched-peptone plate half-seeded with *E. coli* OP50. The worms were allowed to chemotax for 2-4 hours and motile *unc-29(-)* animals were harvested.

RNA capture and sequencing

sRNA

Small RNA (sRNA) was extracted from frozen tissue with the mirVana miRNA Isolation Kit (Ambion). Small RNA libraries were created using a protocol similar to previous miRNA [1, 2] and sRNA capture procedures. All RNA from mirVana isolation was ligated to either Linker-1 or Linker-2 (IDT) in the absence of ATP with T4 RNA ligase 1 (New England Biolabs). Ligated RNA was size selected (38-46nt DNA/RNA hybrid) on 12% PAGE and treated with Antarctic phosphatase (New England Biolabs) to remove all phosphates from the 5' end. The RNA was then treated with T4 polynucleotide kinase (T4 PNK, New England Biolabs) to phosphorylate hydroxylated 5' ends. The 5' ends of T4 PNK-treated RNA were ligated to barcoded adapters as previously described [1]. Dual-ligated RNA was reverse transcribed, PCR amplified and size selected on

4% NuSieve (Lonza) agarose. All sequencing was performed on the Illumina/GAII platform. The following oligos were used:

3' adapters (5' adenylation, 3' dideoxyC):

IDT Linker-1 – rAppCTGTAGGCACCATCAATC

IDT Linker-2 – rAppCACTCGGGCACCAAGGAC

5' adapters (i.e. AF-PP-339, 4nt barcode at 3' end):

/5AmMC6/ ACGCTCTTCCGATCTrArCrUrU

RT oligos:

AF-JX-9 (reverse complement of IDT Linker-1) – ATTGATGGTGCCTACAC

AF-JX-73 (reverse complement of IDT Linker-2) – TCCTTGGTGCCCGAGTG

PCR oligos:

AF_WOL_SOL_FWD – GATACGGCGACCACCGAGATCTACACTCTTTCCCTACACGACGCTCTTCCGATCT

AF_WOL_SOL_REV (for use with IDT Linker-1) – CAAGCAGAAGACGGCATACGAGCTCTTCCGATCTATTGATGGTGCCTACAG

AF_WOL_SOL_REV_2 (for use with IDT Linker-2) – CAAGCAGAAGACGGCATACGAGCTCTTCCGATCTTCCTTGGTGCCCGAGTG

mRNA

mRNA sequencing libraries were prepared using a similar protocol to that of sRNA libraries. High molecular weight (HMW, >200nt) RNA was isolated from frozen tissues with the mirVana miRNA Isolation Kit (Ambion). PolyA(+) RNA was selected from HMW RNA with the MicroPoly(A) Purist Kit (Ambion). The polyA(+) mRNA was then fragmented to 100-200nt using RNA Fragmentation Reagents (Ambion). Because fragmentation creates ends (5'-OH, 3'/2'-P) incompatible with the dual-ligation system, the mRNA was treated with T4 PNK in the presence of ATP to create monophosphorylated 5' and hydroxylated 3' ends. The ATP was then removed with illustra Microspin G-25 columns (GE Healthcare) in order to perform ATP-free 3' adapter ligation. 3' and 5' linker ligations, reverse transcription, and PCR were performed as described above. Libraries were size selected on 2% agarose (Invitrogen).

Sequence processing

Sequencing reads (36nt) for all libraries were generated using the Illumina Genome Analyzer II. Custom Perl scripts were used to identify and remove the 4nt barcode from the 5' end (sRNA and mRNA) and either the linker from the 3' end (sRNA) or the four 3' most bases (mRNA). All sequences were aligned to the *C. elegans* genome and transcriptome (Wormbase release WS190) using BLAT [3] alignment software (sRNA: stepSize=4, tileSize=8; mRNA: stepSize=5, tileSize=11). Sequences were required to meet one of two criteria for inclusion in this study:

1) (a) align perfectly for their whole length (b) be unique to both the genome and transcriptome.

2) align perfectly and uniquely to the transcriptome for their whole length and not align to the genome.

SUPP METHODS TABLE 1

unique_ID	5' BARCODE	3' Linker	AF_SOL	genotype	stage	RNA	cloning protocol	ALL reads with BC and linker	miR	21U	SENSE	ANTISENSE
JMM-cel-001	TTCT	Linker-2	AF_SOL_264_TTCT	ego-1(om84) fem-1(hc17)	L3	sRNA	AP-PNK	2874989	117851	1325	26626	125126
JMM-cel-002	ATAC	Linker-2	AF_SOL_301_ATAC	ego-1(om84) fem-1(hc17)	L3	sRNA	AP-PNK	9566905	479915	1707	29795	82924
JMM-cel-003	GCAG	Linker-2	AF_SOL_264_GCAG	fem-1(hc17)	L3	sRNA	AP-PNK	3565186	308301	3256	66338	364003
JMM-cel-004	GCAG	Linker-2	AF_SOL_281_GCAG	fem-1(hc17)	L3	sRNA	AP-PNK	3167729	474756	3767	63452	446379
JMM-cel-005	CAAT	Linker-2	AF_SOL_230_CAAT	ego-1(om84) fem-1(hc17)	L4	sRNA	AP-PNK	4181720	819830	45882	52762	377799
JMM-cel-006	CAAT	Linker-2	AF_SOL_265_CAAT	ego-1(om84) fem-1(hc17)	L4	sRNA	AP-PNK	4862322	950103	17972	72340	408828
JMM-cel-007	TTCT	Linker-2	AF_SOL_230_TTCT	fem-1(hc17)	L4	sRNA	AP-PNK	7317807	1301154	10236	142532	1165311
JMM-cel-008	ATAC	Linker-2	AF_SOL_265_ATAC	fem-1(hc17)	L4	sRNA	AP-PNK	5116231	821383	32094	75328	660187
JMM-cel-009	GTTA	Linker-1	AF_SOL_119_GTTA	ego-1(om84) fem-1(hc17)	AD	sRNA	AP-PNK	2213814	68437	12868	25081	598044
JMM-cel-010	AAGA	Linker-2	AF_SOL_241_AAGA	ego-1(om84) fem-1(hc17)	AD	sRNA	AP-PNK	1470658	717	2051	19584	271232
JMM-cel-011	TGAA	Linker-2	AF_SOL_244_TGAA	ego-1(om84) fem-1(hc17)	AD	sRNA	AP-PNK	6234606	528019	67042	93600	2131011
JMM-cel-012	TATG	Linker-1	AF_SOL_119_TATG	fem-1(hc17)	AD	sRNA	AP-PNK	1663607	43052	3523	18348	547776
JMM-cel-013	TGAA	Linker-2	AF_SOL_241_TGAA	fem-1(hc17)	AD	sRNA	AP-PNK	811775	649	108	16778	226330
JMM-cel-014	AAGA	Linker-2	AF_SOL_244_AAGA	fem-1(hc17)	AD	sRNA	AP-PNK	6308433	511812	15873	122874	1711739
JMM-cel-015	AAGA	Linker-2	AF_SOL_270_AAGA	ego-1(om84) fem-1(hc17)	L3	mRNA	RNAseq	2754545	-	-	1037801	2253
JMM-cel-016	TATG	Linker-2	AF_SOL_286_TATG	ego-1(om84) fem-1(hc17)	L3	mRNA	RNAseq	4776595	-	-	951766	4473
JMM-cel-017	ACTT	Linker-2	AF_SOL_270_ACTT	fem-1(hc17)	L3	mRNA	RNAseq	5931359	-	-	413413	13148
JMM-cel-018	ACTT	Linker-2	AF_SOL_286_ACTT	fem-1(hc17)	L3	mRNA	RNAseq	5478481	-	-	1612666	4089
JMM-cel-019	ATAC	Linker-2	AF_SOL_239_ATAC	ego-1(om84) fem-1(hc17)	L4	mRNA	RNAseq	7812141	-	-	3494807	13670
JMM-cel-020	TGAA	Linker-2	AF_SOL_271_TGAA	ego-1(om84) fem-1(hc17)	L4	mRNA	RNAseq	3482947	-	-	1318708	2718
JMM-cel-021	TTCT	Linker-2	AF_SOL_239_TTCT	fem-1(hc17)	L4	mRNA	RNAseq	7654390	-	-	3713808	15390
JMM-cel-022	TATG	Linker-2	AF_SOL_271_TATG	fem-1(hc17)	L4	mRNA	RNAseq	2687587	-	-	1857432	7143
JMM-cel-023	ATAC	Linker-1	AF_SOL_132_ATAC	ego-1(om84) fem-1(hc17)	AD	mRNA	RNAseq	3613507	-	-	765757	2836
JMM-cel-024	GCAG	Linker-1	AF_SOL_132_GCAG	ego-1(om84) fem-1(hc17)	AD	mRNA	RNAseq	3091292	-	-	599272	6595
JMM-cel-025	GCAG	Linker-2	AF_SOL_201_GCAG	ego-1(om84) fem-1(hc17)	AD	mRNA	RNAseq	5263220	-	-	2527019	7017
JMM-cel-026	GCAG	Linker-2	AF_SOL_204_GCAG	ego-1(om84) fem-1(hc17)	AD	mRNA	RNAseq	4984860	-	-	2449654	6734
JMM-cel-027	CAAT	Linker-1	AF_SOL_132_CAAT	fem-1(hc17)	AD	mRNA	RNAseq	2771578	-	-	631034	1396
JMM-cel-028	TTCT	Linker-1	AF_SOL_132_TTCT	fem-1(hc17)	AD	mRNA	RNAseq	3429679	-	-	981989	1749
JMM-cel-029	ATAC	Linker-2	AF_SOL_201_ATAC	fem-1(hc17)	AD	mRNA	RNAseq	4599831	-	-	2040160	5532
JMM-cel-030	ATAC	Linker-2	AF_SOL_204_ATAC	fem-1(hc17)	AD	mRNA	RNAseq	5487152	-	-	2498616	6227
JMM-cel-031	TATG	Linker-2	AF_SOL_202_TATG	ego-1(om84) fem-1(hc17)	AD	sRNA	5P-DEP	5786238	2950678	190198	45504	52110
JMM-cel-032	TATG	Linker-2	AF_SOL_205_TATG	ego-1(om84) fem-1(hc17)	AD	sRNA	5P-DEP	3049557	1587112	109273	26496	30888
JMM-cel-033	TGAA	Linker-2	AF_SOL_203_TGAA	ego-1(om84) fem-1(hc17)	AD	sRNA	5P-DEP	2452743	1279815	189415	17359	51494
JMM-cel-034	TGAA	Linker-2	AF_SOL_206_TGAA	ego-1(om84) fem-1(hc17)	AD	sRNA	5P-DEP	3092167	1613987	247329	22883	66673
JMM-cel-035	ACTT	Linker-2	AF_SOL_202_ACTT	fem-1(hc17)	AD	sRNA	5P-DEP	4947750	2554605	58312	59749	142984
JMM-cel-036	ACTT	Linker-2	AF_SOL_205_ACTT	fem-1(hc17)	AD	sRNA	5P-DEP	4134210	2247560	51316	53631	125872
JMM-cel-037	AAGA	Linker-2	AF_SOL_203_AAGA	fem-1(hc17)	AD	sRNA	5P-DEP	4232670	2245104	66106	42682	127356
JMM-cel-038	AAGA	Linker-2	AF_SOL_206_AAGA	fem-1(hc17)	AD	sRNA	5P-DEP	3670612	1953736	60959	37528	114345

Supplementary Methods Table 1. Summary of *ego-1* sequencing. Strains and cloning strategy details can be found in Methods. AP-PNK: Antarctic phosphatase and T4 polynucleotide kinase-treated; 5P-DEP: 5'-monophosphate-dependent; BC: barcode. Counts for miR, 21U, SENSE and ANTISENSE (cDNA) are total sequencing reads that match perfectly to the appropriate reference data set.

SUPP METHODS TABLE 2

GEO accession #/FIRE_name	genotype	raw reads	reads with 3' linker	SENSE	ANTISENSE
GSM454000	CSR-1:IP	3850599	2483976	33358	741579
GSM454001	control animals for CSR-1:IP	4992022	3873256	25496	528234
GSM454002	*csr-1(tm892)*	5139346	4041500	67567	713287
GSM454003	*ego-1(om97)*	5064237	2603976	51010	290730
GSM454004	DA1316	5903016	4586212	47962	753452
GSM455387	control animals for *drh-3(ne4253)* and *ekl-1(tm1599)*	3059030	2197574	13655	330312
GSM455388	control animals for *drh-3(ne4253)* and *ekl-1(tm1599)*	3070842	2254729	17255	430275
GSM455389	*drh-3(ne4253)*	5088634	3381777	34860	46589
GSM455390	*drh-3(ne4253)*	5029803	3402272	42948	56058
GSM455403	*ekl-1(tm1599)*	5529284	2977832	70776	43025
GSM503821	*N2 (for rrf-3; rrf-1; eri-1)*	1863263	1647270	25554	539837
GSM503822	*N2 (for dcr-1; ergo-1)*	2191221	1664919	40215	237917
GSM503823	*rrf-3(pk1426)*	2466605	1830800	26048	648524
GSM503824	*rrf-3(pk1426)*	2512391	2301267	42323	1028592
GSM503825	*rrf-1(pk1417)*	2928625	2377106	40592	904420
GSM503828	*eri-1(mg366)*	1590129	1396626	29135	484562
GSM503830	*ergo-1(gg098)*	3393918	2544374	93163	317863
GSM503831	*dcr-1(mg375)*	3883979	3243322	79126	398993
AF_SOL_287_AGCG	*N2 (for rde-1; rde-4; rrf-1 glp-4; WM126)*	4514797	3495900	53079	1201514
AF_SOL_287_ACTT	*rde-1(ne300)*	4317957	3178834	84542	1017400
AF_SOL_287_CGTC	*rde-4(ne299)*	4459362	3134550	44443	965045
AF_SOL_287_CTGG	*rrf-1(pk1417) glp-4(bn2)*	4893019	3585787	95365	150559
AF_SOL_288_GGGT	MAGO (WM126)	4035150	2072460	42855	371165

Supplementary Methods Table 2. Summary of referenced sequencing. Referenced sequences: name, genotype, number of raw reads, reads with 3' linker. SENSE and ANTISENSE (cDNA) are total sequencing reads that match perfectly to the appropriate reference data set.

Statistics

RNA abundance differences

A Bayesian model was used to determine P-values for sRNA and mRNA abundance levels. This model uses two hypotheses for P-value calculations. The first model assumes that two samples have the same probability for yielding a positive instance for a given gene and the second model assumes that each sample has a unique probability for yielding a positive instance for a given gene. Given a gene in two samples:

Sample 1: P_1 = positive instances for given gene, T_1 = total instances (all genes) in sample

Sample 2: P_2 = positive instances for given gene, T_2 = total instances (all genes) in sample

Therefore, the estimated positive instance value for the first model is given by:

$(P_1+P_2)/(T_1+T_2)$ = PC (combined probability)

and the probability of the observed pattern is given by:

$PROB_{1st}$ = [PC^P_1] * [PC^P_2] * [(1-PC)^(T_1-P_1)] * [(1-PC)^(T_2-P_2)].

The estimated positive instance values for the second model are given by:

Sample 1: $P_1/T_1 = PC_1$

Sample 2: $P_2/T_2 = PC_2$

and the probability of the observed pattern in the second model is given by:

$PROB_{2nd} = [(PC_1 \text{^} P_1) * (PC_2 \text{^} P_2)] * [(1-PC_1) \text{^} (T_1-P_1) * (1-PC_2) \text{^} (T_2-P_2)]$.

The final probability is given by:

$PROB_{final} = PROB_{1st} / PROB_{2nd}$.

Binomial distributions for UP or DOWN

A median value of fold change was calculated for given stage-specific mRNA datasets. Genes whose sRNA abundance were calculated to be significantly different for a given stage were isolated in these mRNA datasets and binomial distributions were calculated for the total number of genes above and below the median value. One-tailed tests were used to determine the appropriate P-value because we had an expectation that genes whose sRNA abundance decreased in an *ego-1(-)* background would show an increase in the abundance of mRNA in an *ego-1(-)* background and vice versa.

Binomial distributions for RNAi mutants

Five median values of the ratio of mutant to control were calculated:

1) all genes
2) only genes with mutant+control counts > 25

3) only genes with mutant+control counts > 200

4) using only genes with mean incidence > $2.5x10^{-4}$

5) using only genes with mean incidence > $2.5x10^{-5}$

* Mean incidences were calculated as $C_A/C_T + M_A/M_T$

(C_A = counts for gene A in control, C_T = total counts for all genes in control, M_A = counts for gene A in mutant, M_T = total counts for all genes in mutant).

Binomial distribution for genomic location of EGO-1-dependent small RNAs

Genome was divided into 100bp bins and the small RNA counts for each bin were tabulated and a fold-change between experimental and control samples was calculated. Examining the 40 bins with the largest fold-change between experimental and control animals, we found that 34 bins spanned an annotated exon. Using those bases that fall into exons throughout the genome, we calculated an observed frequency of bins that should span an annotated exon and from their calculated a binomial distribution for our 100bp bins.

Referenced sequences

Sequences for *csr-1(tm892)* (GSM454002), *ego-1(om97)* (GSM454003), control animals (DA1316) for *csr-1(tm892)* and *ego-1(om97)* (GSM454004), CSR-1:IP (GSM454000), control animals for CSR-1:IP (GSM454001), were obtained from the Gene Expression Omnibus (GEO) [4] accession number GSE18165 [5]. Sequences for *drh-3(ne4253)* (GSM455389 and GSM455390), *ekl-1(tm1599)* (GSM455403), and control animals for *drh-3(ne4253)* and *ekl-1(tm1599)*

(GSM455387 and GSM455388) were obtained from GEO accession number GSE18215 [6]. Sequences for N2 (GSM503821, GSM503822), *rrf-3(pk1426)* (GSM503823, GSM503824), *rrf-1(pk1417)* (GSM503825), *eri-1(mg366)* (GSM503828), *dcr-1(mg375)* (GSM503831), and *ergo-1(gg098)* (GSM503830) were obtained from GEO accession number GSE19414 [7]. Sequences for *rde-1(ne300)*, *rde-4(ne299)*, *rrf-1(pk1417) glp-4(bn2)*, and MAGO (WM126) were obtained from Julia Pak (personal communication). Sequence information can be found in Supp Methods Table 2.

Accession numbers

Illumina raw sequencing reads have been deposited in the NCBI Short Read Archive, accession numbers: GSE26579 (mRNA), GSE26580 (5'-monophosphate-dependent), GSE26581 (5'-monophosphate-independent). Sequence information can be found in Supp Methods Table 1.

SUPPLEMENTARY REFERENCES

1. Gent, J. I., Schvarzstein, M., Villeneuve, A. M., Gu, S. G., Jantsch, V., Fire, A. Z., and Baudrimont, A. (2009). A *Caenorhabditis elegans* RNA-directed RNA polymerase in sperm development and endogenous RNA interference. Genetics *183*, 1297-1314.

2. Lau, N. C., Lim, L. P., Weinstein, E. G., and Bartel, D. P. (2001). An abundant class of tiny RNAs with probable regulatory roles in *Caenorhabditis elegans*. Science *294*, 858-862.

3. Kent, W. J. (2002). BLAT--the BLAST-like alignment tool. Genome Res *12*, 656-664.

4. Edgar, R., Domrachev, M., and Lash, A. E. (2002). Gene Expression Omnibus: NCBI gene expression and hybridization array data repository. Nucleic Acids Res *30*, 207-210.

5. Claycomb, J. M. et al. (2009). The Argonaute CSR-1 and its 22G-RNA cofactors are required for holocentric chromosome segregation. Cell *139*, 123-134.

6. Gu, W. et al. (2009). Distinct argonaute-mediated 22G-RNA pathways direct genome surveillance in the *C. elegans* germline. Mol. Cell *36*, 231-244.

7. Gent, J. I., Lamm, A. T., Pavelec, D. M., Maniar, J. M., Parameswaran, P., Tao, L., Kennedy, S., and Fire, A. Z. (2010). Distinct phases of siRNA synthesis in an endogenous RNAi pathway in *C. elegans* soma. Mol. Cell *37*, 679-689.